

Detecting Regional Lung Properties using Audio Transfer Functions of the Respiratory System

K. Mulligan, A. Adler, *Member IEEE*, and R. Goubran, *Senior Member IEEE*

Abstract — In this study, a novel instrument has been developed for measuring changes in the distribution of lung fluid the respiratory system. The instrument consists of a speaker that inputs a 0 – 4kHz White Gaussian Noise (WGN) signal into a patient’s mouth and an array of 4 electronic stethoscopes, linked via a fully adjustable harness, used to recover signals on the chest surface. The software system for processing the data utilizes the principles of adaptive filtering in order to obtain a transfer function that represents the input – output relationship for the signal as the volume of fluid in the lungs is varied. A chest phantom model was constructed to simulate the behavior of fluid related diseases within the lungs through the injection of varying volumes of water. Tests from the phantom model were compared to healthy subjects. Results show the instrument can obtain similar transfer functions and sound propagation delays between both human and phantom chests.

I. INTRODUCTION

The accumulation of lung fluid or a collapsed lung requires respiratory support for patient stability and treatments such as: antibiotics, puffers, chest tubes, etc. to cure the disease. Often respiratory support augments risks of complications attributable to the endotracheal tube, positive pressure ventilation, or sedation¹. It is difficult to rank the effectiveness of administered treatments without verification through imaging methods such as Computed Tomography (CT) or Magnetic Resonance Imaging (MRI) scans². It has been discovered that lung protective ventilation strategies can be used to drastically improve patient health and reduce Ventilation Induced Lung Injury (VILI)¹. Thus an instrument capable of monitoring the respiratory system would prove to be beneficial.

In this paper, a novel medical instrument has been developed to measure changes in the distribution of lung fluid to aid in the development of lung protective ventilation strategies and to provide physicians with a more immediate method of

verifying the effectiveness of administered lung treatments. The key design focus is to monitor the spatial distribution and relative volume change of lung fluid as treatments are administered into a patient.

The lung monitoring system involves both hardware and software components. For hardware, an array of four electronic stethoscopes was embedded into a fully adjustable harness allowing for attachment to a phantom or human chest. A funnel was attached to a speaker (subwoofer) such that an input sound could be injected into the mouth. The sound signals were measured by the stethoscope array and analyzed through software to calculate indices of regional lung ventilation parameters. This contribution investigates changes in the system transfer function with the presence of increased mucus density within the respiratory system using the instrument.

II. METHODOLOGY

In this section, instrument hardware system configuration, chest phantom construction, and data processing techniques are described.

A. Instrument Hardware Configuration

The construction of the instrument involved two stages: sound emission and capture. In order to emit sound, a speaker (subwoofer) directed sound into a region such as a human mouth through a funnel attached to the end of the speaker. To avoid sounds leaking from the speaker, the speaker was wrapped in 1 inch foam. For sound capture, an array of 4 stethoscopes were attached to a pre-amplifier connected to a fire-wire port of a laptop computer. Figure 1 illustrates a diagram of the 9 off the shelf components required to build the instrument.

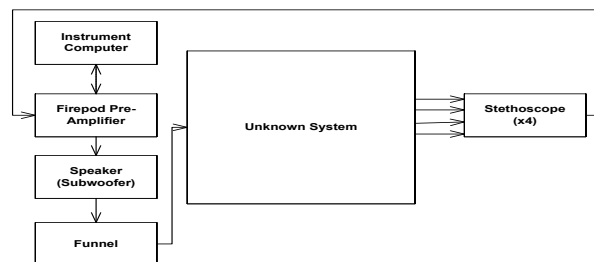


Figure 1 - Block Diagram of the 9 Off The Shelf Components Used to Build the Instrument

This project was funded by the Natural Sciences and Engineering Research Council (NSERC)

K. R. Mulligan is with the Department of Systems and Computer Engineering, Carleton University, Ottawa, ON K1S 5B6 CANADA (e-mail: kmulliga@sce.carleton.ca).

A. Adler, is with the Department of Systems and Computer Engineering, Carleton University, Ottawa, ON K1S 5B6 CANADA. (e-mail: adler@sce.carleton.ca).

R. A. Goubran is with the Department of Systems and Computer Engineering, Carleton University, Ottawa, ON K1S 5B6 CANADA, (e-mail: goubran@sce.carleton.ca).

Following preliminary testing of the system, a harness was developed such that the stethoscope array could be attached to both phantom and human chests. The harness was constructed using nylon straps. Two 1 inch straps with length adjusters were cut to form shoulder straps and sewn to a 3 inch nylon strap also with a length adjuster plus a clip for attachment around the torso. A brass pipe clamp was fastened around each stethoscope head and then attached using 1 inch nylon strapping to the torso strap. The stethoscope heads were attached to the torso strap using material to allow for movement of the heads due to varying physiques and thus locations of auscultation points of individual patients. Figure 2 illustrates the completed stethoscope array harness attached to a human chest.



Figure 2 – Anterior and Posterior Views of the Electronic Stethoscope Array Harness Embedded with 4 Stethoscopes Attached to a Human Torso

B. Adaptive Filtering using NLMS

There are many sources inside the chest that produce noise. Without the ability to measure each sound individually, it is difficult to separate each sound in order to focus solely on those related to breathing. Therefore, adaptive filtering was applied treating the chest as a “blackbox” such that anatomical information inside the chest could be ignored.

The signal outputted from the speaker into either the human or phantom chest to be measured by the stethoscope array was White Gaussian Noise (WGN) spanning from 0- 4kHz. After recovering the input sound signal by the electronic stethoscope array, the signal was processed through the pre-amplifier and sampled at 8kHz prior to routing to the laptop. A calibration⁴ was performed to account for sound acquisition equipment delays. Upon completion of the calibration phase, an adaptive filter was used to develop a transfer function for the unknown system. The specified frequency span for the WGN input sound signal was selected to ensure that only relevant frequencies would be included in the system transfer function.

The system was modeled as a linear adaptive Finite Impulse Response (FIR) filter that used the Normalized Least Mean

Squares (NLMS) algorithm to update its coefficients. The NLMS update algorithm updates the FIR filters coefficients using equation 1.

$$w[n + 1] = w[n] + 2\mu e[n]I[n] \quad (1)$$

where $w[n]$ is the coefficient vector, μ is the step size, $e[n]$ is the error vector, and $I[n]$ is the input vector. An illustration of the adaptive filtering structure employed in this project is shown in Figure 3, where $y_c(n)$ is the signal measured using the electronic stethoscope array and $y_m(n)$ is the signal approximated by the adaptive filter. The overall goal was to iterate the adaptive filtering process updating the adaptive filter (Model) coefficients at each iteration in order to minimize the error vector $e[n]$ which is the difference between the measured signal and the signal outputted from the Model.

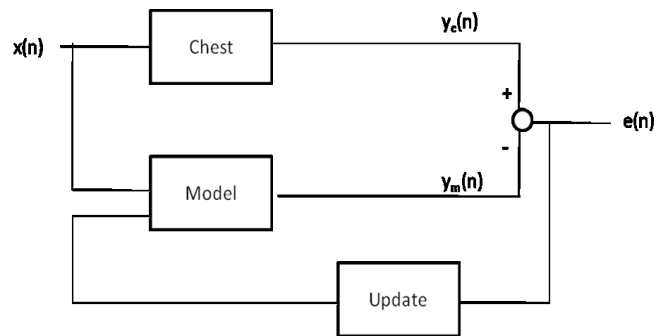


Figure 3 - Adaptive Filtering Structure Employed in this Project

C. Transfer Functions

When the mean squared error (MSE) between the measured signal by the stethoscope array and the model is minimized beyond a convergence threshold on the order of 10^{-6} , a model that is expected to represent the behavior of an unknown system is complete. This model provided a set of FIR filter coefficients that were used to create a transfer function. A transfer function is a mathematical representation of the relationship between the input and output of a linear time-invariant (LTI) system³. Using the coefficients of the direct-form FIR adaptive filter, a transfer function can be built knowing that the impulse response of the system is represented by equation 2.

$$H[z] = b_0 + b_1z^{-1} + b_2z^{-2} + \dots \quad (2)$$

where $H[z]$ is the impulse response, b_n is the n^{th} coefficient value of the FIR filter, and z^{-n} is an n^{th} unit delay based on the sampling frequency. Thus the transfer function can be determined by sweeping over a range of frequencies (typically $0 - \pi$ rads/sample) which changes the value of the delay element z .

D. Chest Phantom Model

A chest phantom model was constructed in order to validate both the hardware and software aspects of the instrument. The chest phantom was constructed using: camping foam ($\rho = 0.01875 \text{ g/cm}^3$), pipe insulation, a tire inner tube, clear tubing, and a syringe. The camping foam was rolled to form a cylinder with a diameter of 0.12 meters and a length of 0.52 meters and held in a cylindrical position using hot glue. The pipe insulation was cut to form two tubes with a diameter and length of 0.04 meters and 0.3 meters respectively. The tubes were inserted into one end of the camping foam at equidistance's from the edge of the camping foam at approximately 0.05 meters. A Y-Pipe was constructed by gluing two 0.1 meter pieces of pipe insulation onto a 0.16 meter piece of pipe insulation and attached to the ends of the tubes. After removing the valve from the tire inner tube stem, the tire tube was slipped over the camping foam cylinder 0.3 meters from the top edge. A 1.8 meter clear piece of tubing with a syringe inserted at one end was attached to the tire stem. Figure 4 illustrates the completed chest phantom model with the electronic stethoscope array appended around the tire tube. The stethoscope harness is able to attach to both a chest phantom model and a human chest⁴.

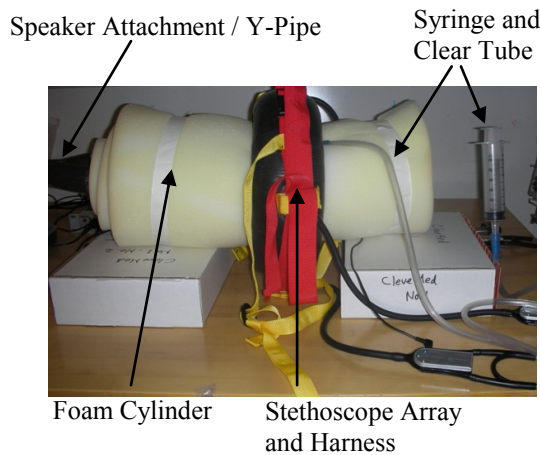


Figure 4 - Chest Phantom Apparatus with the Electronic Stethoscope Array Attached

E. Experimental Procedure (Chest Phantom)

Validation of the system was performed by injecting known volumes of water into the tire inner tube and running the system by playing the input signal using the subwoofer and measuring it with the stethoscope array. Volumes started from 0 cc to 40 cc with an increment of 5 cc per trial and each trial was performed 195 times in order to carry out ensemble averaging which is typical for the NLMS algorithm.

Due to gravity, water injected into the tire inner tube flowed

to the bottom as seen in Figure 5. Furthermore, the speed of sound in water (1500 m/s) is much faster than in air (343 m/s) and as the volume of water increases in the tube, the lower stethoscope (Figure 5) will detect the input signal faster than the other stethoscopes due to a shortened sound propagation delay.

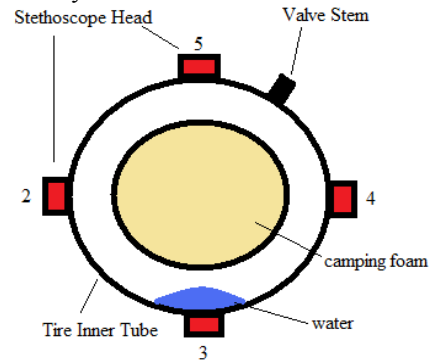


Figure 5 - Illustration of the Stethoscope Array and Inner Tire Tube Assembly. Water Injected into the Tube Flows to the Bottom due to Gravity.

The propagation delay of the input signal can be measured using NLMS adaptive filtering by looking at the coefficient values of the model. The coefficient that has the highest value designates the dominant transmission path of the input signal through the system to the measurement point. Figure 6 shows a plot of the propagation delay of the input signal as water is injected into the tire inner tube. As expected, the delay decreases as the volume of water increases in the tube. The knee in the curve of Figure 6 may be identified with a saturation of water within the sound propagation path of the input sound signal through the tire inner tube. Also, as expected, the propagation delay between the input signal and the other stethoscopes remains constant.

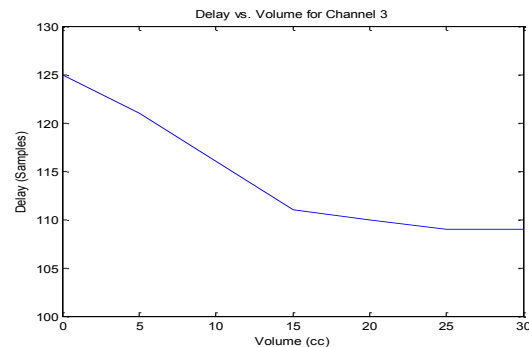


Figure 6 - Plot of the Propagation Delay for the Input Signal to the Stethoscope Attached to Channel 3 of the Pre-Amplifier.

F. Experimental Procedure (Human Chest)

An experiment was performed to compare transfer functions obtained by the chest phantom model and those obtained from human testing. Tests were performed on 3 healthy male subjects between the ages of 20 – 24 in accordance with the

Health Research Ethics Board protocol.

Participants in this experiment were seated in an upright position breathing at tidal volume. The input signal was played and recorded 195 times and the data was run through the NLMS algorithm each time. The model's coefficients upon convergence of the adaptive filtering algorithm were inserted into equation 2 to determine an equation for the impulse response of the system. The impulse response of the system was calculated for a range of frequencies between 0 and π rads/sample and then plotted to reveal the systems transfer function.

III. RESULTS

A. Results (Chest Phantom)

It was observed that with no volume in the chest phantom that the transfer function behaved like a low-pass filter with no DC component. Furthermore, there were two evident frequency spikes at 117.2 Hz and 242.2 Hz. As the volume of injected water into the chest phantom increased, the frequency spikes became sharper. This is illustrated in Figure 7 with a plot showing 3 transfer functions obtained with different volumes of water within the chest phantom model.

The transfer functions shown in Figure 7 are shown for stethoscope labeled 3 in Figure 5 are similar to transfer functions obtained through human trials conducted by K. Ciftci et. al⁵ in which two frequency peaks were also detected in the same frequency range. The next step was to try the instrument on healthy humans to determine if similar behavior to the chest phantom model could be observed.

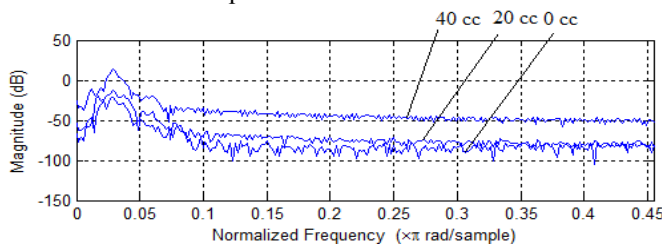


Figure 7 - Above is the magnitude response of the Transfer Function of the Chest Phantom Model with No Volume, 20cc, and 40cc of Water.

B. Results (Human Chest)

The results obtained for each human participant of the experiment were ensemble averaged over all of the 195 trials. Propagation delays in the same range as those measured in the chest phantom model were detected for each participant. Furthermore, two frequency peaks at 86.0 Hz and 171.88 Hz were also observed from the systems transfer function. It was expected that the frequency peaks between

the chest phantom model and the human body would differ due to the material and geometrical differences between the two systems. The resulting transfer functions shown for stethoscope 3 for each participant were constant as the subjects were all healthy and are displayed in Figure 8.

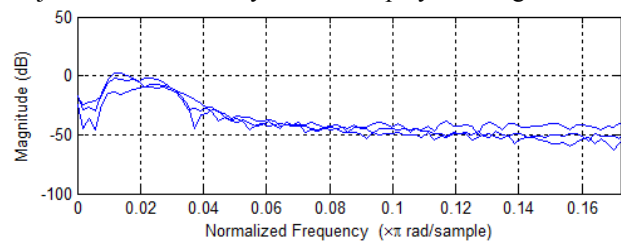


Figure 8 - Transfer Functions for 3 Healthy Human Chests.

IV. DISCUSSION & CONCLUSION

In this paper, the development of a prototype instrument capable of measuring the distribution of lung fluid density within the body was presented. The instrument was tested using a chest phantom model to provide intuitive results of a decaying exponential as the volume of fluid inside the model within the field of view of a stethoscope increased. The transfer function of the chest phantom model showed similar behavior to transfer functions obtained using measurements from real healthy human chests. Further experiments must be conducted on unhealthy humans with fluid related respiratory diseases such as pneumonia, emphysema, asthma, etc. to verify decreases in sound propagation delay, the two peak phenomena inside the transfer function, the smoothing of those peaks as the volume of mucus increases within the respiratory system, and further correlation with the transfer function of the chest phantom model.

V. REFERENCES

- [1] P. Neligan, "Critical Care Medicine Tutorials: All About Oxygen," University of Pennsylvania, <http://www.ccmtutorials.com/rs/oxygen/index.htm>
- [2] J. G. Webster, "Medical Instrumentation: Application and Design," 3rd Edition, *John Wiley & Sons*, New York, Copyright 1998
- [3] G. Birkhoff, G. C. Rota "Ordinary Differential Equations," *John Wiley & Sons*, New York, Copyright 1978
- [4] – K. Mulligan, A. Adler, R. Goubran, "Monitoring Lung Disease using Electronic Stethoscope Arrays," 32nd Annual *Canadian Medical and Biomedical Engineering Conference*, May 20th-22nd 2009, Calgary, AB, Canada, Copyright 2009
- [5] – Adaptive Modeling of Sound Transmission in the Respiratory System
Ciftci, K.; Yeginer, M.; Sen, I.; Cini, U.; Kahya, Y. P. *Engineering in Medicine and Biology Society*, 2004. IEMBS apos:04. 26th Annual International Conference of the IEEE Volume 2, Issue, 1-5 Sept. 2004 Page(s): 3824 - 3827